Harmful Algae 67 (2017) 144–152

Contents lists available at ScienceDirect

Harmful Algae

journal homepage: www.elsevier.com/locate/hal

A method for examining temporal changes in cyanobacterial harmful algal bloom spatial extent using satellite remote sensing

Erin A. Urquhart[a,*], Blake A. Schaeffer[b], Richard P. Stumpf[c], Keith A. Loftin[d], P. Jeremy Werdell[e]

[a] Oak Ridge Institute for Science and Engineering (ORISE), US Environmental Protection Agency, 109 TW Alexander Dr., Durham, NC 27711, USA
[b] National Exposure Research Laboratory, US Environmental Protection Agency, 109 TW Alexander Dr., Durham, NC 27711, USA
[c] National Oceanic and Atmospheric Administration, National Centers for Coastal Ocean Science, 1305 E. West Hwy, Silver Spring, MD 20910, USA
[d] US Geological Survey, Organic Geochemistry Research Laboratory, Kansas Water Science Center, 4821 Quail Crest Pl., Lawrence, KS 66049, USA
[e] Ocean Ecology Laboratory, NASA Goddard Space Flight Center, 8800 Greenbelt Rd., Greenbelt, MD 20771, USA

ARTICLE INFO

Article history:
Received 25 January 2017
Received in revised form 26 May 2017
Accepted 3 June 2017
Available online xxx

Keywords:
Harmful algal blooms
Cyanobacteria
Remote sensing
MERIS
Inland waters

ABSTRACT

Cyanobacterial harmful algal blooms (CyanoHAB) are thought to be increasing globally over the past few decades, but relatively little quantitative information is available about the spatial extent of blooms. Satellite remote sensing provides a potential technology for identifying cyanoHABs in multiple water bodies and across geo-political boundaries. An assessment method was developed using MEdium Resolution Imaging Spectrometer (MERIS) imagery to quantify cyanoHAB surface area extent, transferable to different spatial areas, in Florida, Ohio, and California for the test period of 2008 to 2012. Temporal assessment was used to evaluate changes in satellite resolvable inland waterbodies for each state of interest. To further assess cyanoHAB risk within the states, the World Health Organization's (WHO) recreational guidance level thresholds were used to categorize surface area of cyanoHABs into three risk categories: low, moderate, and high-risk bloom area. Results showed that in Florida, the area of cyanoHABs increased largely due to observed increases in high-risk bloom area. California exhibited a slight decrease in cyanoHAB extent, primarily attributed to decreases in Northern California. In Ohio (excluding Lake Erie), little change in cyanoHAB surface area was observed. This study uses satellite remote sensing to quantify changes in inland cyanoHAB surface area across numerous water bodies within an entire state. The temporal assessment method developed here will be relevant into the future as it is transferable to the Ocean Land Colour Instrument (OLCI) on Sentinel-3A/3B missions.

1. Introduction

Cyanobacterial harmful algal blooms (CyanoHAB) impact lakes and estuaries. Freshwater cyanoHABs occur worldwide and are associated with food web alterations, hypoxia (Paerl et al., 2011), human respiratory and skin irritation during recreational activities, and taste and odor of potable water as a result of ingestion (Stewart et al., 2006). Pets, domestic livestock, and wildlife are also affected by exposure to toxins released during blooms (Backer et al., 2013). Cyanobacterial harmful algal blooms are thought to be increasing globally over the past few decades (Paerl and Paul, 2012; Taranu et al., 2015), but little quantitative information is available about the spatial extent and trends of blooms.

Assessment methods are needed at local, regional, national, and global scales to provide relevant information both in regions

Abbreviations: CyanoHAB, cyanobacterial harmful algal bloom; MERIS, Medium Resolution Imaging Spectrometer; WHO, World health Organization; OLCI, Ocean Land Colour Instrument; HELCOM, Helsinki Commission; ESA, European Space Agency; MODIS, Moderate Resolution Imaging Spectroradiometer; CPL, Coastal Plain; NLA, National Lakes Assessment; SJR, St. Johns River; SWF, Southwest Florida; SF, South Florida; WMT, western mountains; XER, xeric; NAP, northern Appalachians; SAP, southern Appalachians; TPL, temperate plains; SAPS, satellite automated processing system; SeaWiFS, Sea-viewing Wide Field-of-view Sensor; SEADAS, SeaWiFS Data Analysis System; SRTM, Shuttle Radar Topography Mission; Rhos, Rayleigh radiance; CI, Cyanobacteria Index; SS, spectral shape; MRL, minimum reporting level; HABHRCA, Harmful Algal Bloom and Hypoxia Research Control Act; CA_S, southern California; CA_C, central California; CA_N, northern California.

* Corresponding author.
E-mail addresses: urquhart.erin@epa.gov (E.A. Urquhart), Schaeffer.blake@epa.gov (B.A. Schaeffer), Richard.stumpf@noaa.gov (R.P. Stumpf), Kloftin@usgs.gov (K.A. Loftin), Jeremy.werdell@nasa.gov (P. J. Werdell).

http://dx.doi.org/10.1016/j.hal.2017.06.001

already experiencing cyanoHABs as well as regions not yet impacted by blooms. Understanding historical trends is important to inform forecasting efforts and reduce uncertainty estimates (Clark et al., 2001). It is necessary to understand the ecology and dynamics of the water body, and to have information on the presence of cyanoHABs to develop effective water management strategies. Information on cyanoHAB location will help water managers to effectively distribute resources to control and manage them. Scalable assessments may permit the development of management objectives over different temporal periods and spatial scales (Suter, 2007). Periodic updates could then be used to benchmark measures of success.

The temporal assessments for cyanoHABs that do exist typically focus on single, relatively large water bodies such as the Baltic Sea, Lake Taihu, Victoria, and Lake Erie (Chen et al., 2003; Duan et al., 2009; Kahru and Elmgren, 2014; Kahru et al., 2016; Verschuren et al., 2002). Some time series analyses suggest continued increases of cyanoHABs, such as in Lake Taihu and Victoria (Duan et al., 2009; Verschuren et al., 2002). A study examining ~200 years of sedimentary evidence combined with decadal-scale monitoring records revealed that cyanobacteria have increased significantly since 1800, and more rapidly since 1945 in north temperate-subarctic lakes (Taranu et al., 2015). The longest time series using satellite imagery exists for the Baltic Sea (Kahru and Elmgren, 2014), connecting cyanoHABs to phosphorus loads (Kahru et al., 2016). Individual lakes may also see increases in blooms. Lake Taihu experienced extended spring and summer blooms from 1987 to 2007 (Duan et al., 2009), and the lake changed from oligo-mesotrophic, with low algal biomass in 1981, to hypertrophic with cyanobacteria bloom dominated conditions until cessation in 1995 after the implementation of a nutrient reduction program (Chen et al., 2003). In Lake Victoria, a palaeolimnological study found that phytoplankton production increased beginning in the 1930s. Diatom blooms eventually gave way to increased cyanobacteria blooms after 1987 due to anthropogenic landscape alteration (Verschuren et al., 2002). Lake Erie has seen a reappearance of blooms from the 1990s into this century, with more severe blooms in recent years (Stumpf et al., 2012; Wynne and Stumpf, 2015).

Cyanobacterial harmful algal bloom progression is known to be affected by weather patterns and other environmental conditions, natural and anthropogenic (Michalak et al., 2013; Paerl et al., 2011;

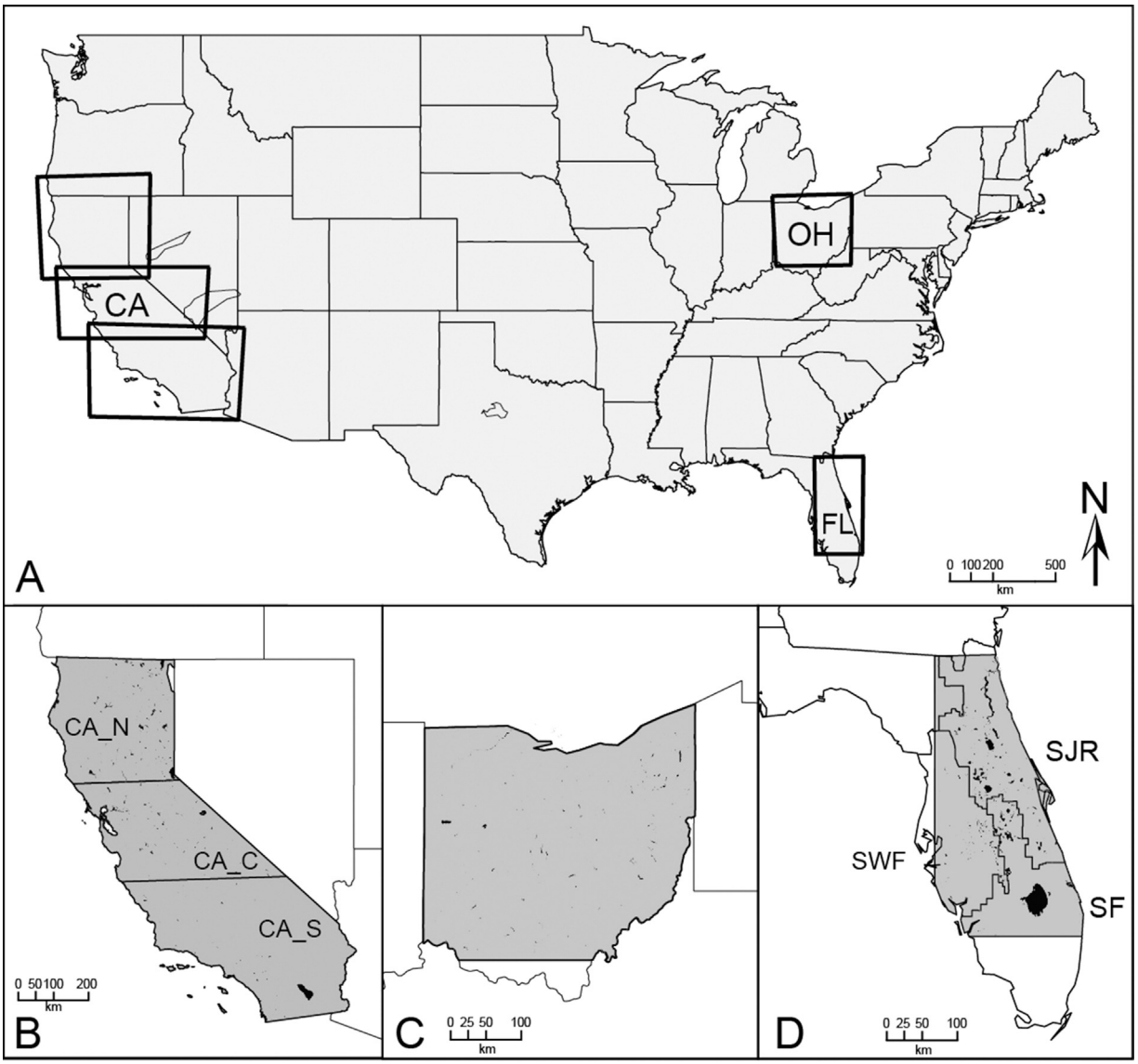

Fig. 1. Study area location map indicating all MERIS scene boundaries (A), California (B), Ohio (C), and Florida with three water management districts (D): St. Johns River (SJR), South West Florida (SWF), and South Florida (SF).

Stumpf et al., 2012). Increased anthropogenic nutrient inputs have been documented as a major driver of cyanoHABs (Downing et al., 2001; Paerl and Otten, 2013). Additional drivers known to promote cyanoHAB growth included changes in the frequency and timing of extreme weather events (Michalak et al., 2013; Paerl and Huisman, 2009), increased water temperature (Kosten et al., 2012), and alterations in water residence time (Elliott, 2010). As a result, studies show variable trends in cyanoHABs. For example, inter-annual variability has been seen in the Baltic Sea. Kahru and Elmgren (2014) found decadal-scale oscillations in extent of cyanobacteria biomass between 1979 and 2013. The Baltic Marine Environment Protection Commission Helsinki Commission (HELCOM) found similar year-to-year variability, while also identifying areas where biomass decreased between 1990 and 2014 (Wasmund et al., 2015). Lake Erie cyanobacteria bloom biovolume varied tremendously after 2002 (Bridgeman et al., 2013; Stumpf et al., 2016). Trends in cyanoHABs are poorly resolved due to the lack of historical *in situ* sample collection and comparable analytical approaches over relevant spatial and temporal extents.

Given the global scope of cyanoHABs (Paerl et al., 2011), relatively few studies of cyanoHABs exist to assess frequency, extent, and duration (Wells et al., 2015). Effective assessment requires more comprehensive data sets than can typically be obtained from field sampling programs. While advances have been made using *in situ* sensor-based collection, these systems provide poor resolution of spatial variability (Foster et al., 2017). The ideal approach would remove these barriers to spatial and temporal assessment and be flexible enough to have sufficient data density to evaluate environmental condition across multiple scales. The need for improved multi-scale assessment capability is desirable so that comparisons and evaluation of condition can occur across local, regional and national scales to more adequately evaluate a nation's water quality, biological integrity, and management actions in a timely, standardized, and cost-effective manner. Investigators have started using satellite data, such as those from the European Space Agency's (ESA) MEdium Resolution Imaging Spectrometer (MERIS) and Ocean and Land Colour Instrument (OLCI) and NASA's Moderate Resolution Imaging Spectroradiometer (MODIS), to evaluate trends in cyanoHABs in different water bodies (Duan et al., 2009; Gómez et al., 2011; Kahru and Elmgren, 2014; Kahru et al., 2016; Matthews and Odermatt, 2015; Palmer et al., 2015; Stumpf et al., 2012; Wynne and Stumpf, 2015).

Satellite data can be used to effectively quantify cyanoHABs, and the highest abundances can be identified (Wynne et al., 2008) on a routine basis for multiple water bodies across geo-political boundaries. In this study, a previously validated algorithm (Lunetta et al., 2015) was selected with the objective of developing a robust temporal assessment method using MERIS. MEdium Resolution Imaging Spectrometer data were used to quantify changes in cyanoHAB surface area extent in lakes in Florida, Ohio, and California. This study was restricted to four years as continuous full resolution MERIS imagery was only available between 2008 and 2012. The 2008 to 2012 MERIS archive may be the best historical record as a relative baseline for comparison against future events to determine change over time given the potential future availability of the operational Senintel-3 OLCI sensors starting in 2017. For the purpose of this study (or method demonstration), cyanoHAB seasonality, duration, and frequency were not assessed.

2. Material and methods

2.1. Study sites

Florida and Ohio study areas were chosen for analysis as they were included in previous satellite cyanobacteria algorithm validation efforts (Lunetta et al., 2015). The state of California was included to assess the extent of cyanoHABs on the western area of the US (Fig. 1). Water bodies that were too narrow to be viewed without overwhelming adjacency effects such as mixed pixels (less than 300 m wide) were excluded. Estuaries and ocean waters were also excluded due to the spectral reflectance of inland lakes and reservoirs differing from the reflectance of coastal estuaries.

The MERIS scene extent for Florida is located within the Coastal Plain (CPL) ecoregion. North of Lake Okeechobee, the climate is subtropical, with hot and humid, high precipitation summers and mild, drier winters (US Climate Data, 2016). The bounding box for Florida only included water bodies located near or within the St. Johns River water management district (SJR), the Southwest Florida water management district (SWF), and the South Florida water management district (SF; Fig. 1D). Based on the findings from the 2007 US Environmental Protection Agency National Lakes Assessment (NLA), lakes in the entire CPL ecoregion have moderate risk to cyanobacteria and cyanotoxins, with 35% microcystin presence (US EPA, 2009).

California is made up of two ecoregions: the western mountains (WMT) and the xeric (XER) west. California's climate varies substantially from mild, rainy winters, and dry warm summers in the coastal and southern portions of the state, to the cold winters and hot summers in the inland semi-arid parts of the state. Northern California generally receives more precipitation than the south, yet overall summer has low rainfall (US Climate Data, 2016). Moderate El Niño-Southern Oscillation (ENSO) events in 2008 and 2009 brought higher than average temperatures and more precipitation to southern California. In 2010, ENSO shifted to La Niña bringing more precipitation to northern California, while southern California remained cool and dry (Seager et al., 2015). The study period preceded the extreme drought of 2012–2014 (Griffin and Anchukaitis, 2014; Swain et al., 2014). Lakes in the WMT ecoregion had lower cyanotoxin risk than other ecoregions (US EPA, 2009). Based on *in situ* cyanobacteria cell counts, 96 percent of lakes within WMT had low microcystin (US EPA, 2009).

The Ohio inland lakes and water bodies (Fig. 1B) used in this study intersect several level III EPA ecoregions: the northern Appalachians (NAP) in the northeast part of the state, the southern Appalachians (SAP) in the south, and the temperate plains (TPL) in the northwest. Ohio's climate is temperate, with cold winters and hot and humid summers. Precipitation is moderate year-round (US Climate Data, 2016). Ninety-five percent of lakes in the NAP ecoregion had low cyanobacteria and cyanotoxins. Microcystin was present in 9% of NAP surveyed lakes. Approximately a quarter (25%) of lakes in the SAP ecoregion had moderate risk levels to cyanobacteria and cyanotoxins exposure, with 25% microcystin presence (US EPA, 2009). Lake Erie was excluded from this study because other programs, such as the NOAA Lake Erie HAB Forecast System, already focused on the Great Lakes (Stumpf et al., 2012; Wynne and Stumpf, 2015).

2.2. Satellite data and processing

The MERIS sensor was selected because of its public availability, spectral range to support deriving cyanobacteria concentrations, 2–4 day return period, and similarities to OLCI (launched February 2016), which can be used for contemporary and future assessments. A total of 5535 full resolution (300 m [m] at nadir) MERIS scenes were obtained for the study areas in three states for 2008 to 2012. Data were processed using the National Oceanic and Atmospheric Administration's (NOAA) satellite automated processing system (SAPS), which incorporates the National Aeronautics and Space Administration (NASA) standard satellite processing software l2gen (packaged within Sea-viewing Wide Field-of-view

Sensor (SeaWiFS) Data Analysis System [SeaDAS] 7.1) and the Shuttle Radar Topography Mission (SRTM) static land mask. Images were separately projected to Universal Transverse Mercator (UTM) using nearest neighbor interpolation. The core output product from l2gen was spectral surface albedo corrected for Rayleigh radiance, $Rhos_{(\lambda)}$. Clouds were masked using an albedo threshold algorithm that accounts for turbid water and excludes pixels with bright reflectances so as not to incorrectly mask intense blooms. Land adjacent pixels were detected when $Rhos_{(885)}$ exceeded $Rhos_{(709)}$, $Rhos_{(754)}$, and 0.01 over pixels identified as water, hereon referred to as resolvable water. This ensured the signals originating from land vegetation were excluded from water pixels. After the masks were applied, the Cyanobacteria Index (CI) was calculated using a spectral shape (SS) algorithm where the second derivative around 665, 681, and 709 nm relates to chlorophyll absorption at 681 as detailed in Wynne et al. (2008). At 681 nm, eukaryotes fluoresce strongly, leading to increased apparent reflectance that obscures the chlorophyll absorption. As cyanobacteria fluoresce poorly (Seppälä et al., 2007), the CI captures the chlorophyll absorption at 681 nm, thereby detecting phytoplankton and excluding many eukaryotes (Stumpf et al., 2016; Wynne et al., 2008). For additional discrimination, a similar approach using 620, 665, and 681 nm was used to identify the presence of phycocyanin (Lunetta et al., 2015; Matthews and Odermatt, 2015), with a positive value indicating moderate to high phycocyanin, a common indicator pigment for cyanobacteria. Remote sensing of phycocyanin is less sensitive than chlorophyll-*a* for estimating cyanobacteria blooms (Stumpf et al., 2016), so the inclusion of the SS(665) criteria may not identify some WHO low-risk cyanobacterial blooms. The MERIS CI output for each image was then converted to cyanobacteria abundance (cells/mL) following Wynne et al. (2010), where cyanoHAB abundance = 1.0×10^8*CI

Monthly maximum temporal composites were computed instead of mean composites to minimize the effect of clouds or wind that might otherwise reduce detection of the bloom. Monthly maximums of cyanoHAB surface area coverage may provide conservative overestimation, however sensitivity analysis of cloud cover percentage (results not shown) revealed that weekly and ten-day composites still had gaps in detection. Many cyanoHAB species such as *Microcystis*, *Aphanizomenon*, and *Dolichospermum*, have buoyancy control and will typically float to the surface in the day during calm wind (Visser et al., 2015). Strong winds can mix the blooms into the water column, diluting the surface concentration seen by the satellite (Wynne et al., 2010). Over one month, the cells would be near the surface on one or more days (Stumpf et al., 2012; Wynne and Stumpf, 2015). For cyanobacteria that have limited buoyancy control, this method will quantify the monthly maximum surface concentration.

Extensive field validation of the CI algorithm was previously demonstrated in Florida, Ohio, and the New England states (Lunetta et al., 2015; Tomlinson et al., 2016). Lunetta et al. (2015), revised by Clark et al. (2017), report correspondence across the spectrum of cyanoHAB abundance ranges spanning 10,000 to >1 million cells/mL (mean absolute percentage error, MAPE = 28.6%, coefficient of determination, $R^2 = 0.95$). Satellite derived values below 109,000 cells/mL and above 1,000,000 cells/mL had correspondence of above 80% with *in situ* samples collected within 7± days of a satellite match up. While the CI algorithm had lower correspondence performance between 109,000–1,000,000 cells/mL, this was expected due to the lack of validation data in this concentration range and the large temporal range for coincident satellite match-ups. The categorization of satellite derived CI values based on WHO recreational guidance levels, as described below, would further reduce the impact on algorithm error and uncertainties.

2.3. Change estimation and evaluation

All statistical analyses were conducted using the R Statistical Environment (R Core Team, 2015), version 3.2.0. Temporal assessment of area coverage of water affected by a cyanoHAB was computed for each of the three selected states. The area coverage (km^2) of cyanoHAB in each monthly composite was calculated as the number of resolvable water pixels multiplied by the native spatial resolution (300 m × 300 m) of the sensor. This area was then normalized by the study area of resolvable water for each state, resulting in the percent of detectable area per image. Minimum reporting level (MRL) or detectable cyanoHAB was defined as pixels which have cyanobacteria abundance >10,000 cells/mL (Lunetta et al., 2015). Following the WHO recreational guidance levels thresholds (Chorus and Bartram, 1999) using only cell abundance, area of detectable cyanobacteria bloom was categorized into four categories: (1) low probability of acute health effects (low-risk) with cells/mL < 19,999, (2) moderate probability of acute health effects (moderate-risk) with 19,999 < cells/mL < 99,999, and (3) high probability of acute health effects (high-risk) with cells/mL > 99,999 (Chorus and Bartram, 1999; Graham et al., 2010). Lastly, (4) the total surface bloom area and surface area of non-detectable bloom water was calculated.

The Kendall tau test (Kendall, 1938) and the Theil-Sen estimator for slope (Sen, 1968) were used to assess changes in the surface area over time. Statistical tests for monotonic trend (simple linear regression) in seasonal time series are often confounded by nonnormal data, missing values, detection limits, and serial dependence. The seasonal Kendall provides a nonparametric test for trend computed as the median of the slopes determined by the pair-wise comparison of all sample points within each season (Hirsch and Slack, 1984). A modification of the Theil-Sen estimator for slope (Hirsch and Slack, 1984) provides an unbiased estimator of trend magnitude under conditions of seasonal cycles without assumptions regarding normality, serial dependence, or homoscedasticity of residuals. A positive Kendall's tau value indicates that the rank of the variable increased over time, whereas a negative tau value denoted that as the rank of one variable increased, the other variable decreased with a downward trend (Kendall, 1938). Kendall's tau is inherently smaller than Spearman's rho, however easily interpretable. If 2/3 of the data pairs had an increase with time, tau = 0.5; for equal pairs where 1/2 increased and 1/2 decreased with time, tau = 0.

To assess the magnitude of the trend, the ratio of the variation in the data around the trend line, often referred to as the residual variability, over the slope (km^2/yr) of the time series was determined (hereafter referred to as *Y*) as an effect-size metric analogous to Cohen's d. This metric captures the time required for the trend to exceed the variability. Residual standard error (RSE) was used to account for residual variability. A 95% confidence interval for the Theil-Sen slope across all seasons was also reported. Effect sizes captured the slope against the variability and assessed the magnitude of research findings, information that cannot be obtained with frequentist statistics (Durlak, 2009; Thompson, 2006; Volker, 2006).

2.4. Demonstration of assessment at different spatial scales

Extension of the current methods to smaller spatial domains such as water management districts, watersheds, or to the county level, may be useful to inform stakeholders at scales that interest them. To illustrate the applicability of the methods to differing spatial scales, analysis was applied to the three regions of California: northern California (CA_N), central California (CA_C), and southern California (CA_S; Fig. 1B). Further, the methods outlined above were applied to three Water Management Districts

in the state of Florida: south west Florida (SWF), St. Johns River (SJR), and south Florida (SF; Fig. 1D). Florida's Water Management Districts administer a variety of programs including flood protection, water management plans for water shortages, managing the consumptive use of water and surface water, as well as storm water management (Florida Department of Environmental Protection, 2016).

3. Results

The total surface water area resolvable by MERIS for Florida (650 waterbodies), California (381), and Ohio (257) is 13,794 km^2, 21,289 km^2, and 1876 km^2 respectively. Clouds and the 2–4 day temporal repeatability of MERIS inhibited the production of a continuous time-series. During times of impeding cloud coverage, reduced retrievals and thus reduced accuracy due to the fewer number of scenes with cloud-free pixel data were expected. Fig. 2 illustrates the monthly mean cloud coverage represented as a percent of resolvable water pixels for each study area in Florida, Ohio, and California from 2008 to 2012. Mean monthly percent cloud coverage was calculated using all MERIS scenes prior to temporal binning. Seasonal trends in percent cloud coverage were apparent for each region, with peaks during the winter months and troughs during the summer in California and Ohio. In Florida, seasonal cycles with steady fluctuations in cloud coverage were observed throughout the year. Intra-annual cloud fluctuations, particularly during the summer months, were not surprising as central Florida is characterized by wet, cloudy summers due to its semi-tropical climate.

The total bloom area increased by 215 km^2/yr in Florida (slope in Table 1) from 2008 to 2012. While the total bloom area peaks changed little each year, the troughs increased from 4000 km^2 in 2008 to 5600 km^2 in 2011, a rate of 400 km^2/yr (Fig. 3A). Ohio and California had changes in total area, −0.18 km^2/yr in Ohio, and −13.6 km^2/yr in California, from 2008 to 2012. Bloom area for resolvable water in Florida, Ohio, and California represented as a monthly percentage, illustrated the changes in cyanobacteria in lakes greater than 0.9 km^2 (Fig. 3B). Bloom area encompassed approximately 45–95% of resolvable water area in Florida, 20–45% in California, and 10–90% in Ohio.

Table 1
Time series statistics for non-bloom area (ND), total bloom area (bloom), low-risk bloom area (low), moderate-risk bloom area (mod), and high-risk bloom area (high) in Florida (FL), Ohio (OH), and California (CA). Statistics include: 95% confidence interval for slope, Theil-Sen slope, Kendall's tau, and residual variability/slope (*Y*).

region	WHO	95% CI	slope (km^2/yr)	tau	*Y*
FL	ND	−469.9:−54.3	−255.0	−0.33	3.3
	bloom	−23.9:487.0	215.3	0.28	4.1
	low	−26.8:5.0	−9.90	−0.18	7.8
	mod	−243.8:114.7	−27.7	−0.08	26.4
	high	244.0:849.8	502.8	0.39	1.9
OH	ND	−14.7:7.6	−5.85	−0.17	7.94
	bloom	−13.5.9:12.9	−0.18	0.00	>100
	low	0.0:0.3	0.00	0.25	Inf
	mod	0.03:2.4	0.52	0.36	7.72
	high	−11.7:9.9	−1.65	−0.08	29.4
CA	ND	−19.3.8:256.7	122.1	0.22	2.9
	bloom	−319.7:208.4	−13.6	−0.06	43.9
	low	−0.3:6.1	2.1	0.22	6.5
	mod	−64.2:92.7	7.87	0.08	24.4
	high	−351.0:270.6	−16.7	−0.03	31.9

Highlighting change that was large against the variability in the data, in Florida, high-risk category blooms increased by a rate of 502.8 km^2/yr, approximately 0.03% of total resolvable surface water area in Florida (Table 1). The largest change in Florida occurred in the area of high-risk probability of acute health effects (Fig. 4A). The high-risk bloom (those with cyanobacterial cells/mL > 99,999) troughs nearly doubled from 2008 (∼2000 km^2) to 2012 (∼4000 km^2). Ohio had negligible surface area change in high-risk areas (Fig. 4B). California may have seen a slight decrease in high-risk area (Fig. 4C, −16.7 km^2/yr) from 2008 to 2012, but this trend was small relative to the high variability in the dataset (Table 1, *Y* = 32 years).

Central California exhibited an increase (31.12 km^2/yr) in total bloom area that was moderate against the data variability (*Y* = 5.4 years; Table 2). The change in CA_C was likely attributed to the change in area of high-risk blooms (19.6 km^2/yr), however this trend was small relative to the variability in the high-risk time series (*Y* = 7.9 years). Additionally, moderate-risk blooms (ranging from 20,000–99,999 cells/mL) may have increased (11.4 km^2/yr) as the change was moderate relative to the variability in the data (*Y* = 4.8 years). Low-risk blooms (less than 20,000 cells/mL) in CA_N

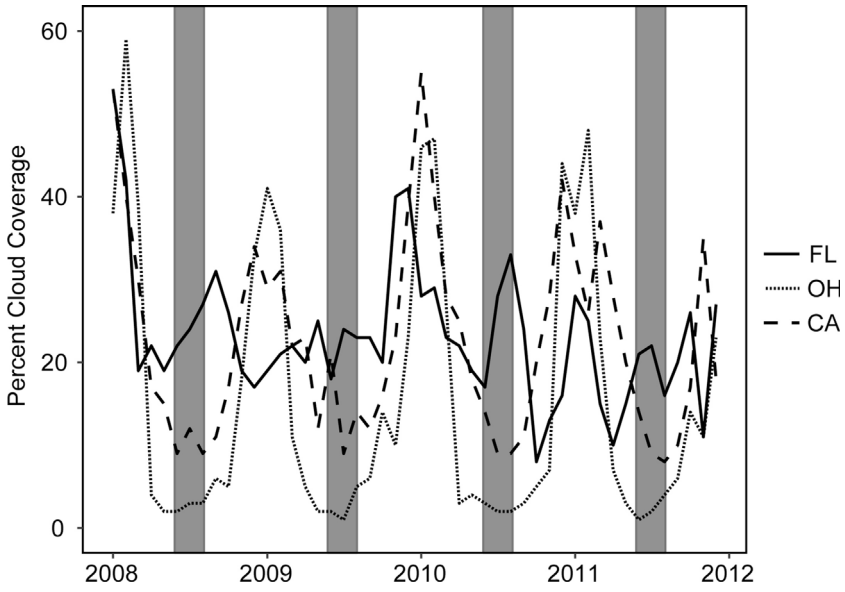

Fig. 2. Percent monthly mean cloud coverage for FL, OH, and CA assessed by satellite and extrapolated from daily MERIS imagery. Shaded regions represent summer months (June–August).

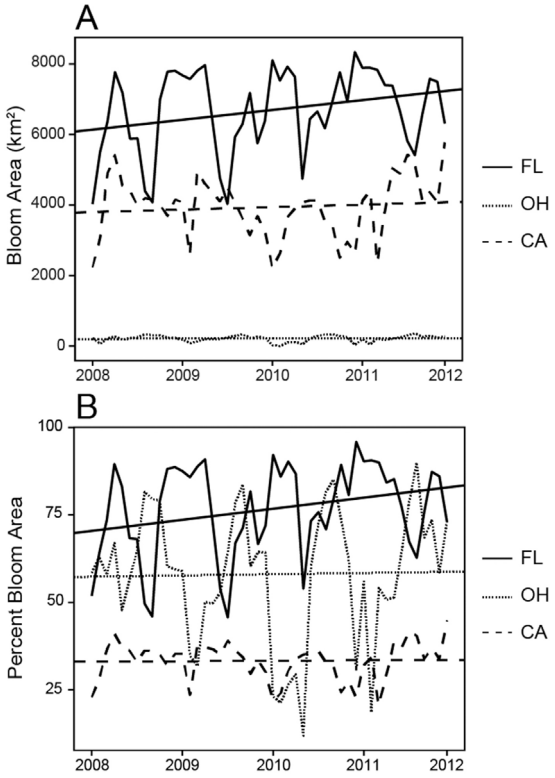

Fig. 3. Monthly temporal assessment of (A) total bloom area (km^2) for FL, OH, and CA, and (B) percent bloom area for resolvable water area in FL, OH, and CA, including linear regression lines.

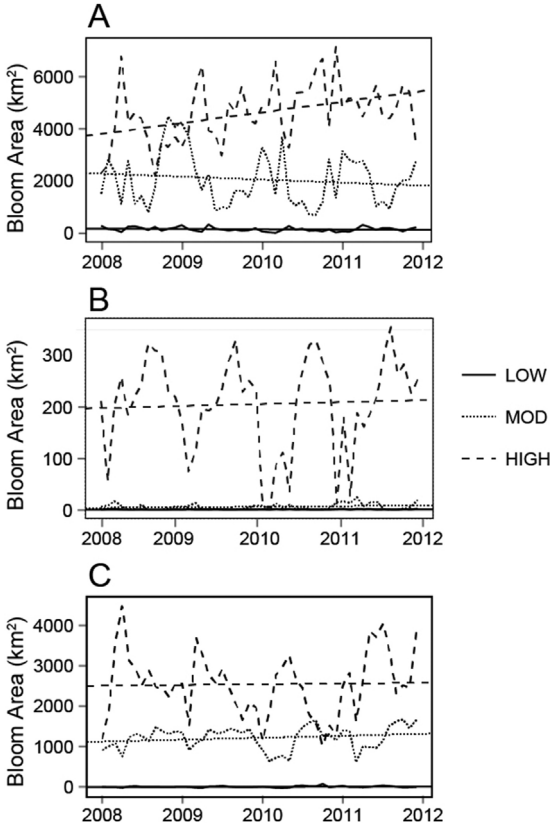

Fig. 4. Times series of bloom area by WHO guidance levels for recreational waters for FL (A), OH (B), and CA (C). TS of low-risk, moderate-risk, and high-risk are indicated by figure legends, including linear regression lines.

Table 2
Time series statistics for Northern California (CA_N), Central California (CA_C), and Southern California (CA_S). Statistics include: 95% confidence interval for slope, Theil-Sen slope, Kendall's tau, and residual variability/slope (*Y*).

region	WHO	95% CI	slope (km^2/yr)	tau	*Y*
CA_N	ND	−21.1:170.1	51.55	0.22	4.7
	bloom	−276.9:184.8	1.14	0.00	>100
	low	0.30:4.3	2.05	0.33	5.2
	mod	−75.7:64.0	11.4	0.03	14.0
	high	−256.3:216.8	−3.8	−0.03	>100
CA_C	ND	−4.3:105.1	37.45	0.27	4.6
	bloom	−9.4:88.5	31.12	0.22	5.4
	low	−1.9:2.4	0.22	0.07	25.6
	mod	−2.5:31.2	11.40	0.22	4.8
	high	−44.2:78.7	19.60	0.11	7.9
CA_S	ND	−20.7:26.1	3.63	0.08	20.6
	bloom	−13.6:27.7	1.2	0.03	67.8
	low	−0.6:0.6	0.13	0.07	28.2
	mod	−7.3:13.6	2.35	0.07	10.3
	high	−19.5:21.8	−1.7	0.00	45.2

Table 3
Time series statistics for the South Florida Water Management District (SF), the St. Johns River Water Management District (SJR), and the South West Florida Water Management District (SWF). Statistics include: 95% confidence interval for slope, Theil-Sen slope, Kendall's tau, and residual variability/slope (*Y*).

region	WHO	95% CI	slope (km^2/yr)	tau	*Y*
SF	ND	−335.4:44.5	−163.50	−0.25	4.2
	bloom	−51.8:298.6	157.42	0.19	4.5
	low	−23.8:19.5	−3.90	−0.08	16.0
	mod	−157.1:206.6	14.92	0.03	40.1
	high	−125.9:534.0	300.00	0.22	2.7
SJR	ND	−178.9:−47.4	−111.45	−0.39	1.9
	bloom	47.6:178.5	112.2	0.39	2.0
	low	−6.9:−0.6	−3.85	−0.38	2.9
	mod	−135.6:−27.4	−63.2	−0.44	3.2
	high	111.0:281:9	179.5	0.61	1.4
SWF	ND	−6.3:8.7	−0.60	−0.06	37.4
	bloom	−7.5:17.4	1.45	0.03	24.7
	low	−0.3:0.0	−0.10	−0.21	6.7
	mod	−3.3:4.8	0.45	0.06	27.7
	high	−6.1:11.1	1.43	0.06	20.5

may have increased slightly (2.05 km^2/yr), but this change was minimal relative to the total resolvable surface water area of 15,730 km^2 in northern California. Further, the decrease observed in CA_N high-risk blooms may have been reason for the slight decrease observed in the state as a whole (Table 2). As northern California encompasses nearly 50% of the satellite resolvable freshwater in the state, changes in the region can impact estimates statewide.

For a smaller spatial applicability, analysis was performed on three water management districts within the state of Florida (Fig. 5). Table 3 presents the maximum monthly results for each water management district derived from the 2008 to 2012 MERIS data. There were bloom area increases in all three water management districts with the largest increases occurring primarily within SJR (Fig. 5C) and SF (Fig. 5D). Total surface bloom area coverage in SJR increased by 112.2 km^2/yr, a strong trend relative to the total variability in the dataset (*Y* = 2 years), and total resolvable surface water area (2787.6 km^2). While the surface bloom area of low-risk and moderate-risk blooms categories has declined in SJR, the high-risk blooms have increased substantially by a rate of 179.5 km^2/yr from 2008 to 2012. Similarly, high-risk blooms in SF, home to Lake Okeechobee (51% of total resolvable water in Florida), have increased by a rate of 300 km^2/yr relative to the 5522.5 km^2 of total resolvable surface water.

4. Discussion

In 2014, Congress reauthorized the Harmful Algal Bloom and Hypoxia Research Control Act (HABHRCA 2014; P.L. 113-124) that focused on issues related to HABs and hypoxia. An interagency HABHRCA report in 2016 identified monitoring challenges, which included sustaining monitoring programs and maintaining consistency of methods across monitoring programs. A specific HABHRCA report recommendation included the ability to strengthen long-term HAB monitoring. The status and assessment approach described in this paper can assist in addressing both the monitoring challenge and recommendation. This work provides an opportunity for each US state to have a uniform satellite dataset (Schaeffer et al., 2015) and a consistent approach for determining the spatial extent and rate of change, year-to-year, with long-term operational satellites. This work advances beyond statements that HABs are generally increasing, and now provide stakeholders and managers quantifiable cyanoHAB rates of change and spatial extent.

Historically, the question of whether or not freshwater cyanoHABs are increasing in frequency, extent, and duration has been addressed by temporal assessments that focus on single water bodies (Cao et al., 2016; Chen et al., 2003; Kahru and Elmgren, 2014; Srifa et al., 2016; Stumpf et al., 2012; Verschuren et al., 2002). Furthermore, focused studies can be limited by their

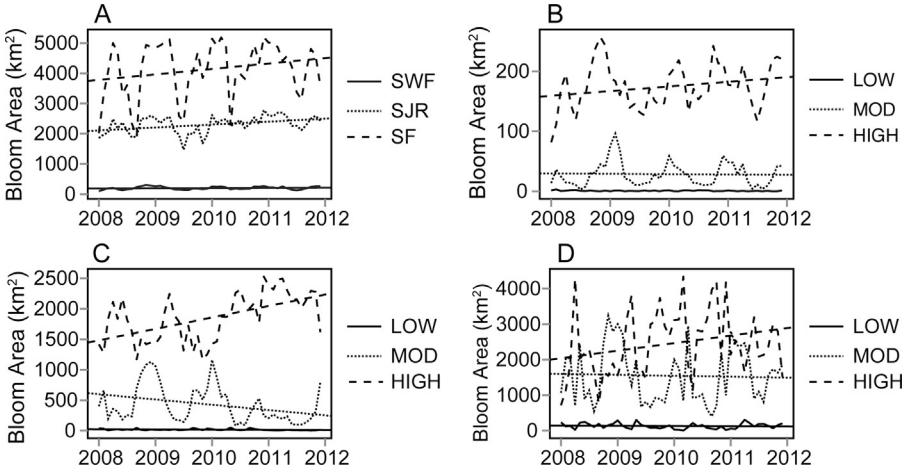

Fig. 5. Temporal assessment of Florida water management districts by surface area of bloom for each WMD (A), and bloom area by risk category for SF (B), SJR (C), and SWF (D), including linear regression lines.

geographic extent leading to the inability to relate cyanoHAB trends to changes in climate, environment, land use, extreme weather events, and the feedbacks of these variables. While satellite data have been limited by temporal resolution and technology, satellite remote sensing remains a powerful tool for providing data where field and *in situ* efforts lack temporal or spatial coverage.

The primary objective of this effort is development of a robust method for examining temporal changes in cyanoHAB spatial extent. To illustrate applicability of the presented assessment methods at varying spatial scales, analysis was performed in three watershed management districts in Florida. High-risk blooms, as defined by WHO, increased Florida by a rate of 502.8 km^2/year, which was likely attributed to the changes within the SJR and SF watershed management districts. Total surface bloom area coverage in SJR increased from 2008 to 2012, attributed primarily to the very large increase in WHO high-risk category. As noted above, even though both WHO low-risk and moderate-risk bloom area in Florida have decreased at minimal rates per year, the trends have the potential to be environmentally meaningful over a ten-year period. South Florida, home to the state's largest freshwater lake, Lake Okeechobee, also exhibited increases in WHO-defined high-risk bloom area. Results were consistent with previous findings (Burns, 2008; Chapman and Schelske, 1997) that the occurrence of cyanobacterial blooms in selected Florida waters have become more prominent over time, particularly in many of Florida's largest waterbodies including: Lake Okeechobee, the lower St. Johns River, and the Harris Chain of Lakes in the SJR.

Changes in WHO moderate-risk category remain the most difficult to interpret. If the area with the moderate-risk blooms increased, for example, the question remains as to whether it came at the loss of the total low-risk bloom area, indicating increased concentrations and a more significant problem; or at the loss of a total high-risk bloom area, which indicates an improvement in conditions. Overall increase in low-risk area is, of course, more favorable for managers and stakeholders. Furthermore, trends within WHO guidance levels may be influenced by pixels having values near the thresholds between categories (low, moderate, and high).

While the ability to quantify changes in inland cyanobacteria blooms using satellite data was demonstrated here, it is important to note the operating boundaries of this study. Water bodies that were too narrow to be viewed without land adjacency effects (<300 m wide) were excluded from the assessment. It may be possible that higher resolution sensors such as those on Landsat-8 and Sentinel-2 may provide assessments for smaller water bodies. To address the question of whether individual waterbodies impact overall changes relative to the size of the waterbody, we test the effect by omitting Lake Okeechobee, the largest waterbody in Florida, from the state trend analysis. Excluding Lake Okeechobee from the Florida analysis shows no change in the direction of the slope or the relative effect size (Y) of the trend (Supplementary Table 1). Since the St. Johns River Water Management District was identified to also have a large influence on the changes observed in Florida, a small subset of lakes known to be highly impacted by cyanoHABs (Harris Chain of Lakes and Lake Apopka) was removed from the SJR analysis. Similarly, removing a few specific lakes from the SJR analysis has no effect on the direction of the trend or the effect size (Supplementary Table 2).

Another potential limitation is that wind stress can impact the vertical distribution of a bloom throughout the water column. Often, blooms get stranded at the surface losing their ability to regulate buoyancy in the water column, which can lead to thick, near-shore accumulations. Given the difficulty for satellites to see subsurface and the ability to deconvolute mixed land-water pixels, near-shore accumulations may be misrepresented by satellite imagery causing underestimation of the bloom. Additionally, the depth of light attenuation in the red bands used to detect blooms is related to light intensity, water clarity, and color, approximately equivalent to one secchi depth. In situations, where a bloom is dispersed vertically, the whole lake cell density can be underestimated if the bloom is distributed deeper than approximately one secchi depth (Chorus and Bartram, 1999; Stumpf and Werdell, 2010).

Finally, as targeted MERIS acquisitions with the full resolution sensor are only available between 2002 and 2007, with continuous full resolution acquisition mode available only from 2008 to 2012, the present study was restricted to a four-year time period of 2008 through 2011. That being said, as identified by the calculated residual variability (Y), in most cases, even a longer time series of an arbitrary continuous length of time (for example, 10 full years of MERIS data), may still not provide enough data to discern a trend through the high variability of these datasets. The 2008 to 2012 MERIS archive may be the best historical record as a relative baseline for comparison against future events to determine change over time given the potential future availability of the operational Senintel-3 OLCI sensors starting in 2017. The gap of available assessment data between 2012 and 2017 emphasizes the need for continuity of missions similar to that of the Landsat missions (Schaeffer et al., 2013). The assessment method developed in this study will be relevant into the future as it is transferable to OLCI on Sentinel-3A launched February 2016 and Sentinel–3B scheduled for launch in 2017. These missions will extend the temporal assessment for use in future forecast applications.

This work builds upon the findings from numerous case studies on inland waters by using satellite data to extend trend identification for cyanobacteria blooms to a state scale and across numerous water bodies. Furthermore, by observing the WHO guidance levels for the relative probability of acute health effects during recreational exposure to cyanobacteria as examples, this method will assist in prioritizing the degree of potential exposure risk to cyanobacteria. Results show that overall, surface area extent of cyanoHABs increased in Florida between 2008 and 2012. California exhibited a very slight decrease, mainly attributed to decreases in northern California between 2008 and 2012. Ohio (excluding Lake Erie) exhibited little change in cyanoHABs in all risk categories between 2008 and 2012.

Acknowledgements

This work was supported by the NASA Ocean Biology and Biogeochemistry Program/Applied Sciences Program (proposal 14-SMDUNSOL14-0001) and by U.S. EPA, NOAA, U.S. Geological Survey Toxic Substances Hydrology Program, and Oak Ridge Institute for Science and Technology (ORISE). This article has been reviewed by the National Exposure Research Laboratory and Office of Water and approved for publication. Mention of trade names or commercial products does not constitute endorsement or recommendation for use by the U.S. Government. The views expressed in this article are those of the authors and do not necessarily reflect the views or policies of the U.S. EPA. The authors would like to thank John Darling, John Clark, Elizabeth Hilborn, John Iiames, Ross Lunetta, and Megan VanFossen for many useful comments on the manuscript. Mention of trade names or commercial products does not constitute endorsement or recommendation for use.[CG]

Appendix A. Supplementary data

Supplementary data associated with this article can be found, in the online version, at http://dx.doi.org/10.1016/j.hal.2017.06.001.

References

Backer, L.C., Landsberg, J.H., Miller, M., Keel, K., Taylor, T.K., 2013. Canine cyanotoxin poisonings in the United States (1920s–2012): review of suspected and confirmed cases from three data sources. Toxins 5 (9), 1597–1628.

Bridgeman, T.B., Chaffin, J.D., Filbrun, J.E., 2013. A novel method for tracking western Lake Erie *Microcystis* blooms, 2002–2011. J. Great Lakes Res. 39 (1), 83–89.

Burns, J., 2008. Toxic Cyanobacteria in Florida Waters, Cyanobacterial Harmful Algal Blooms: State of the Science and Research Needs. Springer, pp. 127–137.

Cao, X., Wang, Y., He, J., Luo, X., Zheng, Z., 2016. Phosphorus mobility among sediments, water and cyanobacteria enhanced by cyanobacteria blooms in eutrophic Lake Dianchi. Environ. Pollut. 219, 580–587.

Chapman, A.D., Schelske, C.L., 1997. Recent appearance of *cylindrospemopsis* (Cyanobacteria) in five hypereutrophic florida lakes. J. Phycol. 33 (2), 191–195.

Chen, Y., Qin, B., Teubner, K., Dokulil, M.T., 2003. Long-term dynamics of phytoplankton assemblages: *Microcystis*-domination in Lake Taihu, a large shallow lake in China. J. Plankton Res. 25 (4), 445–453.

Chorus, E.I., Bartram, J., 1999. Toxic Cyanobacteria in Water: a Guide to Their Public Health Consequences, Monitoring and Management. E&FN Spon, London.

Clark, J.S., Carpenter, S.R., Barber, M., Collins, S., Dobson, A., Foley, J.A., Lodge, D.M., Pascual, M., Pielke Jr., R., Pizer, W., 2001. Ecological forecasts: an emerging imperative. Science 293 (5530), 657–660.

Clark, J., Schaeffer, B.A., Darling, J., Urquhart, E., Johnston, J., Ignatius, A., Myer, M., Loftin, K.A., Werdell, P.J., Stumpf, R.P., 2017. Satellite monitoring of cyanobacterial harmful algal bloom frequency in recreational waters and drinking water sources. Ecol. Indic. 80, 84–95.

Downing, J.A., Watson, S.B., McCauley, E., 2001. Predicting cyanobacteria dominance in lakes. Can. J. Fish. Aquat. Sci. 58 (10), 1905–1908.

Duan, H., Ma, R., Xu, X., Kong, F., Zhang, S., Kong, W., Hao, J., Shang, L., 2009. Two-decade reconstruction of algal blooms in China's Lake Taihu. Environ. Sci. Technol. 43 (10), 3522–3528.

Durlak, J.A., 2009. How to select, calculate, and interpret effect sizes. J. Pediatr. Psychol. jsp004.

Elliott, J.A., 2010. The seasonal sensitivity of Cyanobacteria and other phytoplankton to changes in flushing rate and water temperature. Global Change Biol. 16 (2), 864–876.

Florida Department of Environmental Protection, 2016. Water Management Districts. .

Foster, G.M., Graham, J.L., Stiles, T., Boyer, M., King, L.R., Loftin, K.A., 2017. Spatial variability of harmful algal blooms in Milford, Kansas, July and August 2015. US Geological Survey Scientific Investigations Report. , pp. 2016–5168.

Gómez, J.A.D., Alonso, C.A., García, A.A., 2011. Remote sensing as a tool for monitoring water quality parameters for Mediterranean Lakes of European Union water framework directive (WFD) and as a system of surveillance of cyanobacterial harmful algae blooms (SCyanoHABs). Environ. Monit. Assess. 181 (1), 317–334.

Graham, J.L., Loftin, K.A., Meyer, M.T., Ziegler, A.C., 2010. Cyanotoxin mixtures and taste-and-odor compounds in cyanobacterial blooms from the Midwestern United States. Environ. Sci. Technol. 44 (19), 7361–7368.

Griffin, D., Anchukaitis, K.J., 2014. How unusual is the 2012–2014 California drought? Geophys. Res. Lett. 41 (24), 9017–9023.

Hirsch, R.M., Slack, J.R., 1984. A nonparametric trend test for seasonal data with serial dependence. Water Resour. Res. 20 (6), 727–732.

Kahru, M., Elmgren, R., 2014. Multidecadal time series of satellite-detected accumulations of cyanobacteria in the Baltic Sea. Biogeosciences 11 (13), 3619–3633.

Kahru, M., Elmgren, R., Savchuk, O.P., 2016. Changing seasonality of the Baltic sea. Biogeosciences 13 (4), 1009–1018.

Kendall, M.G., 1938. A new measure of rank correlation. Biometrika 30 (1/2), 81–93.

Kosten, S., Huszar, V.L.M., Bécares, E., Costa, L.S., van Donk, E., Hansson, L.-A., Jeppesen, E., Kruk, C., Lacerot, G., Mazzeo, N., De Meester, L., Moss, B., Lürling, M., Nõges, T., Romo, S., Scheffer, M., 2012. Warmer climates boost cyanobacterial dominance in shallow lakes. Global Change Biol. 18 (1), 118–126.

Lunetta, R.S., Schaeffer, B.A., Stumpf, R.P., Keith, D., Jacobs, S.A., Murphy, M.S., 2015. Evaluation of cyanobacteria cell count detection derived from MERIS imagery across the eastern USA. Remote Sens. Environ. 157, 24–34.

Matthews, M.W., Odermatt, D., 2015. Improved algorithm for routine monitoring of cyanobacteria and eutrophication in inland and near-coastal waters. Remote Sens. Environ. 156, 374–382.

Michalak, A.M., Anderson, E.J., Beletsky, D., Boland, S., Bosch, N.S., Bridgeman, T.B., Chaffin, J.D., Cho, K., Confesor, R., Daloğlu, I., 2013. Record-setting algal bloom in Lake Erie caused by agricultural and meteorological trends consistent with expected future conditions. Proc. Natl. Acad. Sci. 110 (16), 6448–6452.

Paerl, H.W., Huisman, J., 2009. Climate change: a catalyst for global expansion of harmful cyanobacterial blooms. Environ. Microbiol. Rep. 1 (1), 27–37.

Paerl, H.W., Otten, T.G., 2013. Harmful cyanobacterial blooms: causes, consequences, and controls. Microb. Ecol. 65 (4), 995–1010.

Paerl, H.W., Paul, V.J., 2012. Climate change: links to global expansion of harmful cyanobacteria. Water Res. 46 (5), 1349–1363.

Paerl, H.W., Hall, N.S., Calandrino, E.S., 2011. Controlling harmful cyanobacterial blooms in a world experiencing anthropogenic and climatic-induced change. Sci. Total Environ. 409 (10), 1739–1745.

Palmer, S.C.J., Kutser, T., Hunter, P.D., 2015. Remote sensing of inland waters: challenges, progress and future directions. Remote Sens. Environ. 157, 1–8.

R Core Team, 2015. R (Software): A Language and Environment for Statistical Computing. Vienna, Austria.

Schaeffer, B.A., Schaeffer, K.G., Keith, D., Lunetta, R.S., Conmy, R., Gould, R.W., 2013. Barriers to adopting satellite remote sensing for water quality management. Int. J. Remote Sens. 34 (21), 7534–7544.

Schaeffer, B.A., Loftin, K.A., Stumpf, R.P., Werdell, P.J., 2015. Agencies collaborate, develop a cyanobacteria assessment network. EOS 96.

Seager, R., Hoerling, M., Schubert, S., Wang, H., Lyon, B., Kumar, A., Nakamura, J., Henderson, N., 2015. Causes of the 2011–14 california drought. J. Clim. 28 (18), 6997–7024.

Sen, P.K., 1968. Estimates of the regression coefficient based on Kendall's tau. J. Am. Stat. Assoc. 63 (324), 1379–1389.

Seppälä, J., Ylöstalo, P., Kaitala, S., Hällfors, S., Raateoja, M., Maunula, P., 2007. Ship-of-opportunity based phycocyanin fluorescence monitoring of the filamentous cyanobacteria bloom dynamics in the Baltic Sea. Estuar. Coast. Mar. Sci. 73 (3–4), 489–500.

Srifa, A., Phlips, E.J., Cichra, M.F., Hendrickson, J.C., 2016. Phytoplankton dynamics in a subtropical lake dominated by cyanobacteria: cyanobacteria 'like it hot'and sometimes dry. Aquat. Ecol. 1–12.

Stewart, I., Webb, P.M., Schluter, P.J., Shaw, G.R., 2006. Recreational and occupational field exposure to freshwater cyanobacteria—a review of anecdotal and case reports, epidemiological studies and the challenges for epidemiologic assessment. Environ. Health 5 (1), 6.

Stumpf, R.P., Werdell, P.J., 2010. Adjustment of ocean color sensor calibration through multi-band statistics. Opt. Express 18 (2), 401–412.

Stumpf, R.P., Wynne, T.T., Baker, D.B., Fahnenstiel, G.L., 2012. Interannual variability of cyanobacterial blooms in Lake Erie. PLoS One 7 (8), e42444.

Stumpf, R.P., Davis, T.W., Wynne, T.T., Graham, J.L., Loftin, K.A., Johengen, T.H., Gossiaux, D., Palladino, D., Burtner, A., 2016. Challenges for mapping cyanotoxin patterns from remote sensing of cyanobacteria. Harmful Algae 54, 160–173.

Suter II, G., 2007. Ecological Risk Assessment. CRC Press, Taylor and Francis Group, Boca Raton.

Swain, D.L., Tsiang, M., Haugen, M., Singh, D., Charland, A., Rajaratnam, B., Diffenbaugh, N.S., 2014. The extraordinary California drought of 2013/2014: character, context, and the role of climate change. Bull. Am. Meteorol. Soc. 95 (9), S3.

Taranu, Z.E., Gregory-Eaves, I., Leavitt, P.R., Bunting, L., Buchaca, T., Catalan, J., Domaizon, I., Guilizzoni, P., Lami, A., McGowan, S., Moorhouse, H., Morabito, G., Pick, F.R., Stevenson, M.A., Thompson, P.L., Vinebrooke, R.D., 2015. Acceleration of cyanobacterial dominance in north temperate-subarctic lakes during the Anthropocene. Ecol. Lett. 18 (4), 375–384.

Thompson, B., 2006. Research synthesis: effect sizes. In: Green, J., Camilli, C., Elmore, P.B. (Eds.), Complementary Methods for Research in Education. American Education Research Association, Washington, DC.

Tomlinson, M.C., Stumpf, R.P., Wynne, T.T., Dupuy, D., Burks, R., Hendrickson, J., Fulton Iii, R.S., 2016. Relating chlorophyll from cyanobacteria-dominated inland waters to a MERIS bloom index. Remote Sens. Lett. 7 (2), 141–149.

US Climate Data, Version 2.2. Accessed November 2, 2016 from http://www.usclimatedata.com/climate/florida/united-states, 2016.

US EPA, 2009. National Lakes Assessment: A Collaborative Survey of the Nation's Lakes. U.S. Environmental Protection Agency, Office of Water and Office of Research and Development, Washington, D.C.

Verschuren, D., Johnson, T.C., Kling, H.J., Edgington, D.N., Leavitt, P.R., Brown, E.T., Talbot, M.R., Hecky, R.E., 2002. History and timing of human impact on Lake Victoria, East Africa. Proc. R. Soc. Lond. B: Biol. Sci. 269 (1488), 289–294.

Visser, P.M., Ibelings, B.W., Bormans, M., Huisman, J., 2015. Artificial mixing to control cyanobacterial blooms: a review. Aquat. Ecol. 1–19.

Volker, M.A., 2006. Reporting effect size estimates in school psychology research. Psychol. Schools 43 (6), 653–672.

Wasmund, N., Busch, S., Gobel, J., Gromisz, S., Hoglander, H., Jaanus, A., Johansen, M., Jurgensone, I., Kownacka, J., Krasniewski, W., Lehtinen, S., Olenina, I., Weber, M., 2015. Cyanobacteria Biomass. HELCOM Baltic Sea Environment Fact Sheet 2015. .

Wells, M.L., Trainer, V.L., Smayda, T.J., Karlson, B.S., Trick, C.G., Kudela, R.M., Ishikawa, A., Bernard, S., Wulff, A., Anderson, D.M., 2015. Harmful algal blooms and climate change: learning from the past and present to forecast the future. Harmful Algae 49, 68–93.

Wynne, T.T., Stumpf, R.P., 2015. Spatial and temporal patterns in the seasonal distribution of toxic cyanobacteria in western Lake Erie from 2002–2014. Toxins 7 (5), 1649–1663.

Wynne, T.T., Stumpf, R.P., Tomlinson, M.C., Warner, R.A., Tester, P.A., Dyble, J., Fahnenstiel, G.L., 2008. Relating spectral shape to cyanobacterial blooms in the Laurentian Great Lakes. Int. J. Remote Sens. 29 (12), 3665–3672.

Wynne, T.T., Stumpf, R.P., Tomlinson, M.C., Dyble, J., 2010. Characterizing a cyanobacterial bloom in western Lake Erie using satellite imagery and meteorological data. Limnol. Oceanogr. 55 (5), 2025–2036.